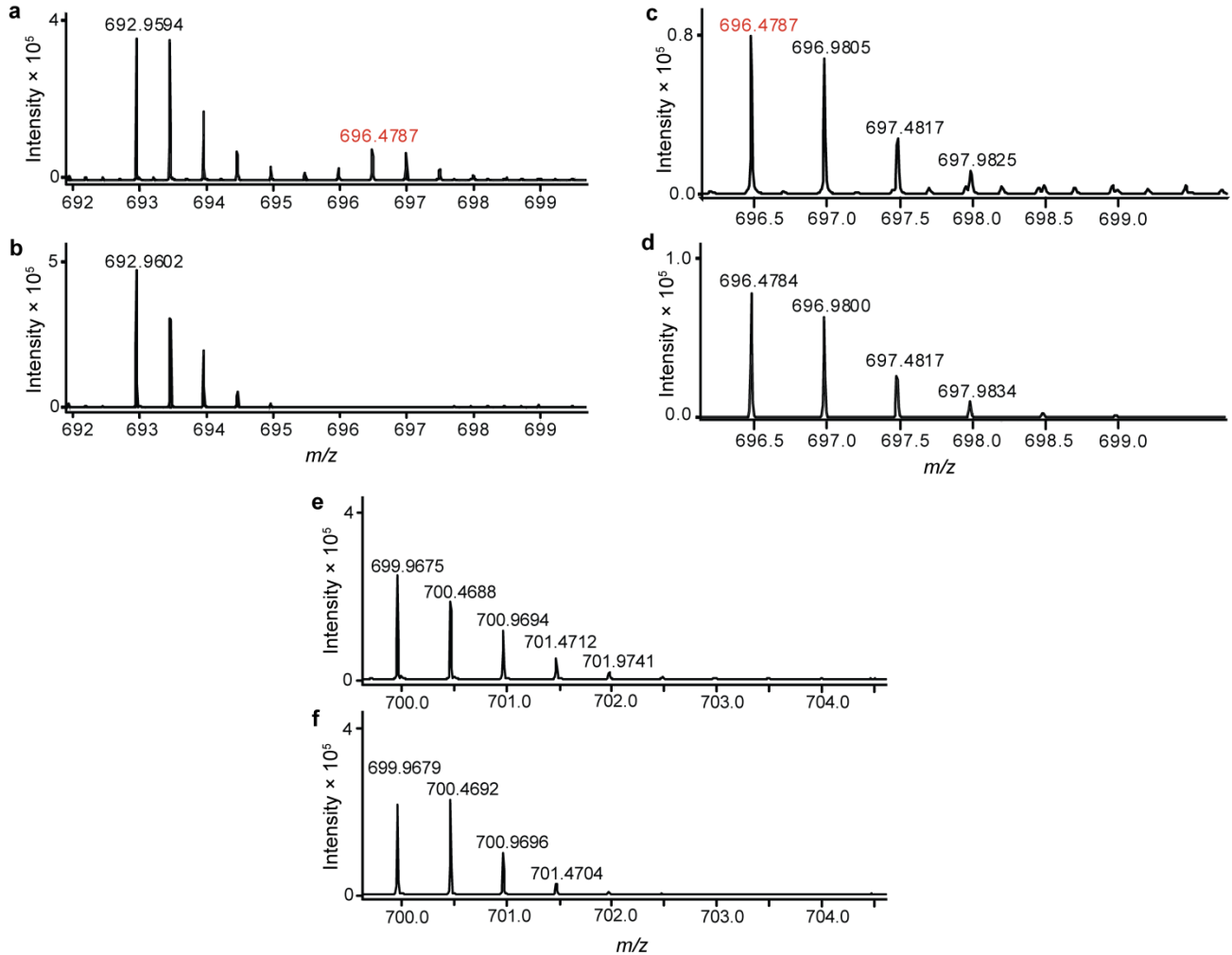
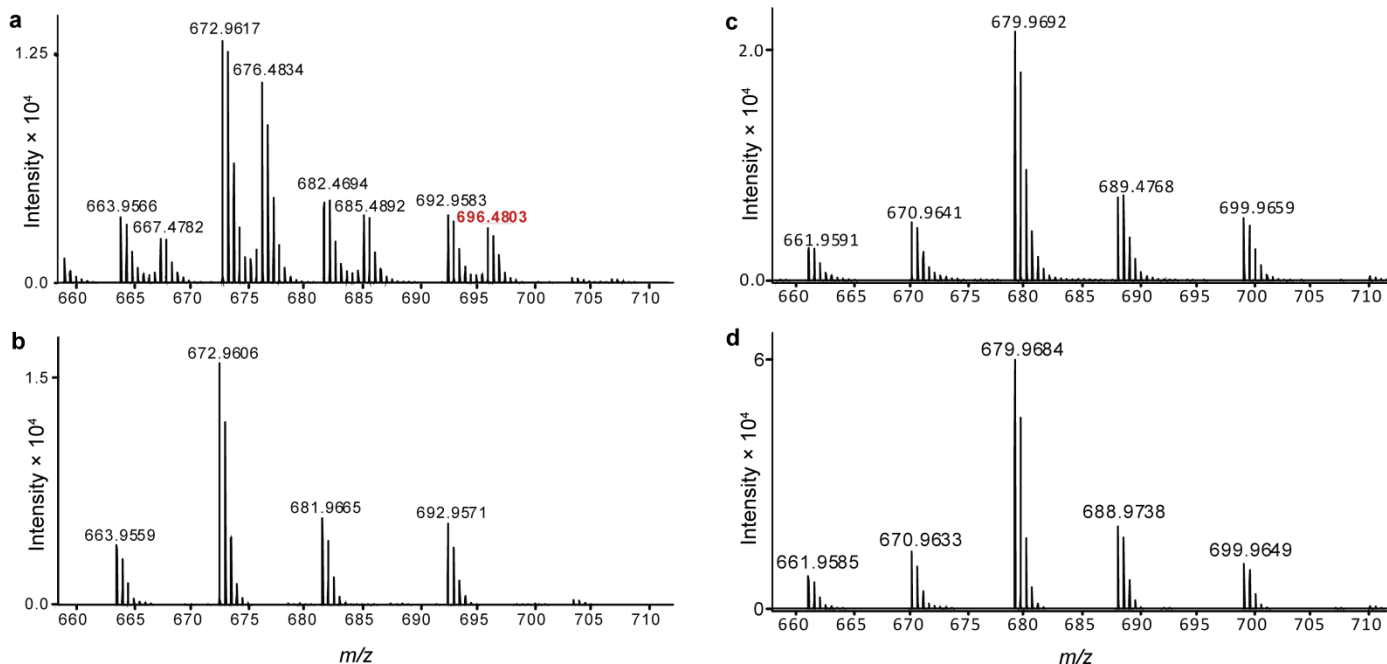


Supplementary Figure 1: Sequence alignment of CCRC homologues identified in *Streptomyces ambofaciens* ATCC23877 with well characterized CCRCs. The residues highlighted by the stars and red boxes are essential in defining the substrate specificity of CCRCs.¹⁻³ The specificity-conferring residues in the CCRC homologues in *S. ambofaciens* ATCC23877 do not resemble those of RevT, PteB, and CinF, all of which are known to be responsible for the biosynthesis of longer alkylmalonyl-CoA extender units. The sequence names highlighted in red are those from *S. ambofaciens* ATCC23877. The sequences designated CCRc and CCR_S are both specific for crotonyl-CoA and the three CCRC homologues in *S. ambofaciens* have very similar specificity-conferring residues to these enzymes. Accession numbers: CCRc, 3HZZ; CCR_S, 3KRT; AntE, AGG37751;

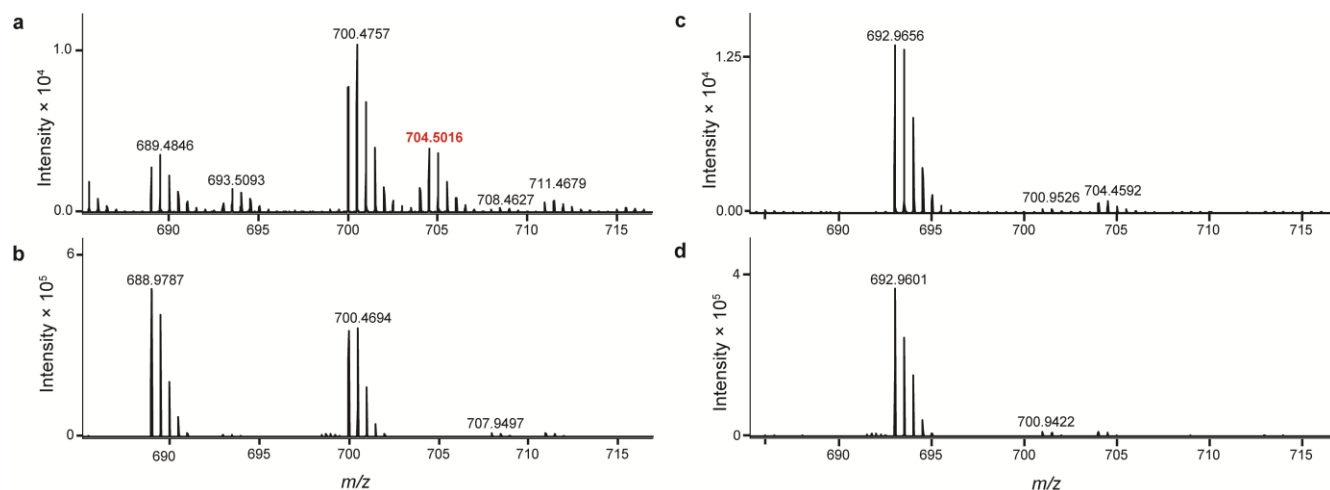
SpnE, AKA54628; PteB, WP_010981851; SalG, ABP73651; RevT, BAK64636; CinF, CBW54676; SamL0374 (SAM23877_0426), AKZ53475; Srm4*c (SAM23877_5633), AKZ58678; SAM23877_6076, AK59112



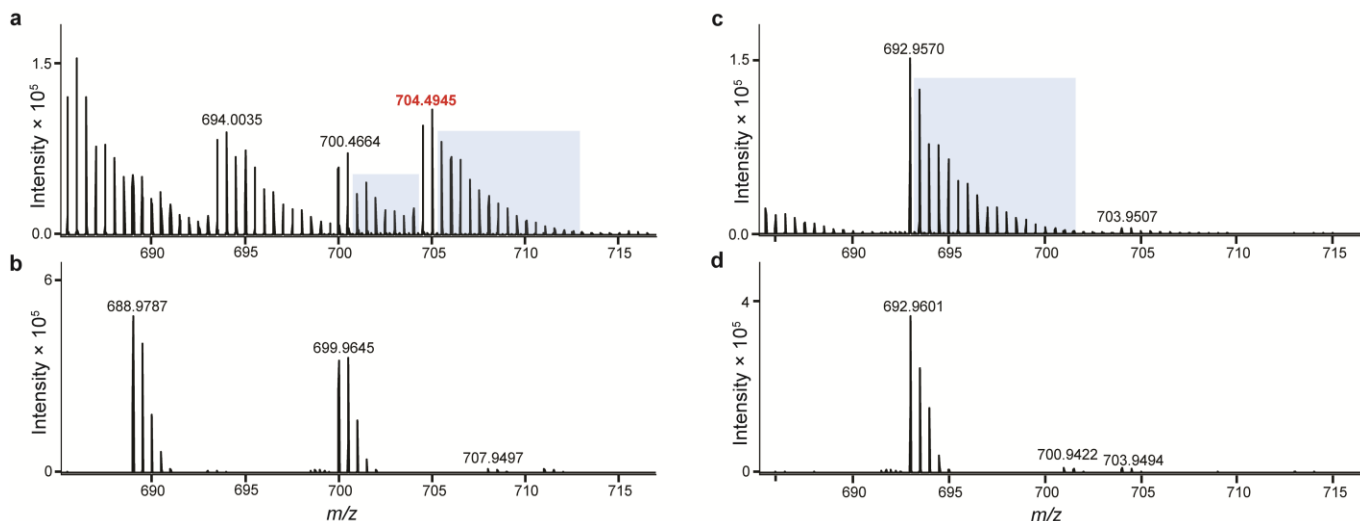
Supplementary Figure 2: Mass spectra from UHPLC-ESI-Q-TOF-MS analysis of methanolic mycelial extracts from the $[U-^2H]$ L-valine 11 incorporation experiments. Spectra resulting from addition of (a) 5 mM $[U-^2H]$ L-valine 11 and (b) no $[U-^2H]$ L-valine to the growth medium. The signal at $m/z = 692.9594$ corresponds to $[M+Na+H]^{2+}$ for stambomycins C/D 3/4 and the signal at $m/z = 696.4787$ corresponds to $[M+Na+H]^{2+}$ for stambomycin C 3 derived from incorporation of $[U-^2H]$ L-valine 11. Comparison of the spectrum (c) measured for labeled stambomycin C 3 derived from incorporation of $[U-^2H]$ L-valine 11 with (d) the spectrum calculated for the $[C_{72}H_{125}D_7NNaO_{22}]^{2+}$ ion. Spectra for stambomycins A/B 1/2 resulting from addition of (e) 5 mM $[U-^2H]$ L-valine 11 and (f) no $[U-^2H]$ L-valine to the growth medium. No specific incorporation of the deuterium-labeled precursor is observed.



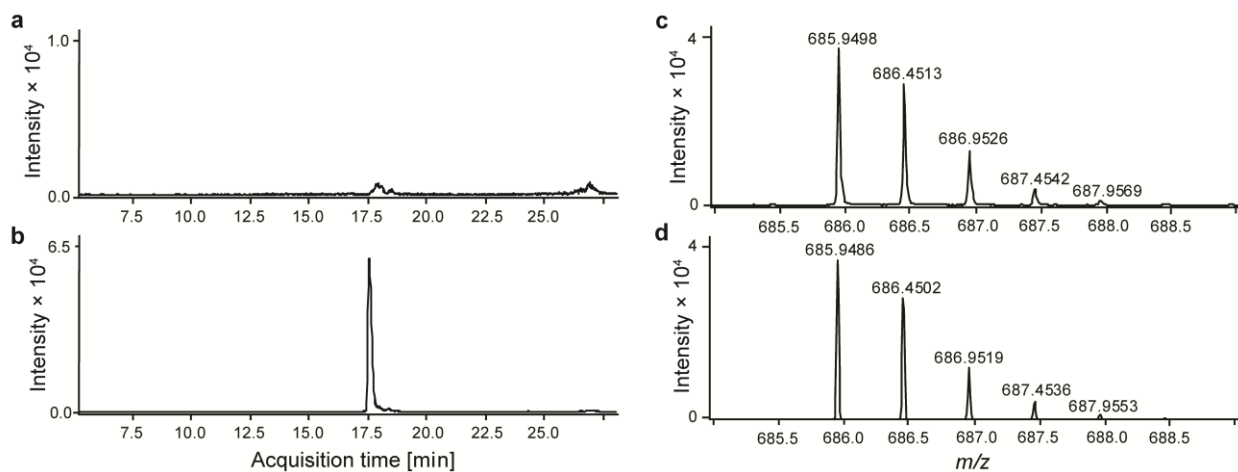
Supplementary Figure 3: Mass spectra from UHPLC-ESI-Q-TOF-MS analysis of methanolic mycelial extracts from the [U- 2 H]butyric acid 12 incorporation experiments. Spectra resulting from addition of (a) 5 mM [U- 2 H]butyric acid 12 and (b) no [U- 2 H]butyric acid to the growth medium. The signal at $m/z = 692.9583$ corresponds to $[M+Na+H]^{2+}$ for stambomycins C/D 3/4 and the signal at $m/z = 696.4803$ corresponds to $[M+Na+H]^{2+}$ for stambomycin D 4 derived from incorporation of [U- 2 H]butyric acid 12 (calculated for $[C_{72}H_{125}D_7NNaO_{22}]^{2+}$:696.4784). Spectra for stambomycins A/B 1/2 resulting from addition of (c) 5 mM [U- 2 H]butyric acid 12 and (d) no [U- 2 H]butyric acid to the growth medium. No specific incorporation of the deuterium-labeled precursor is observed.



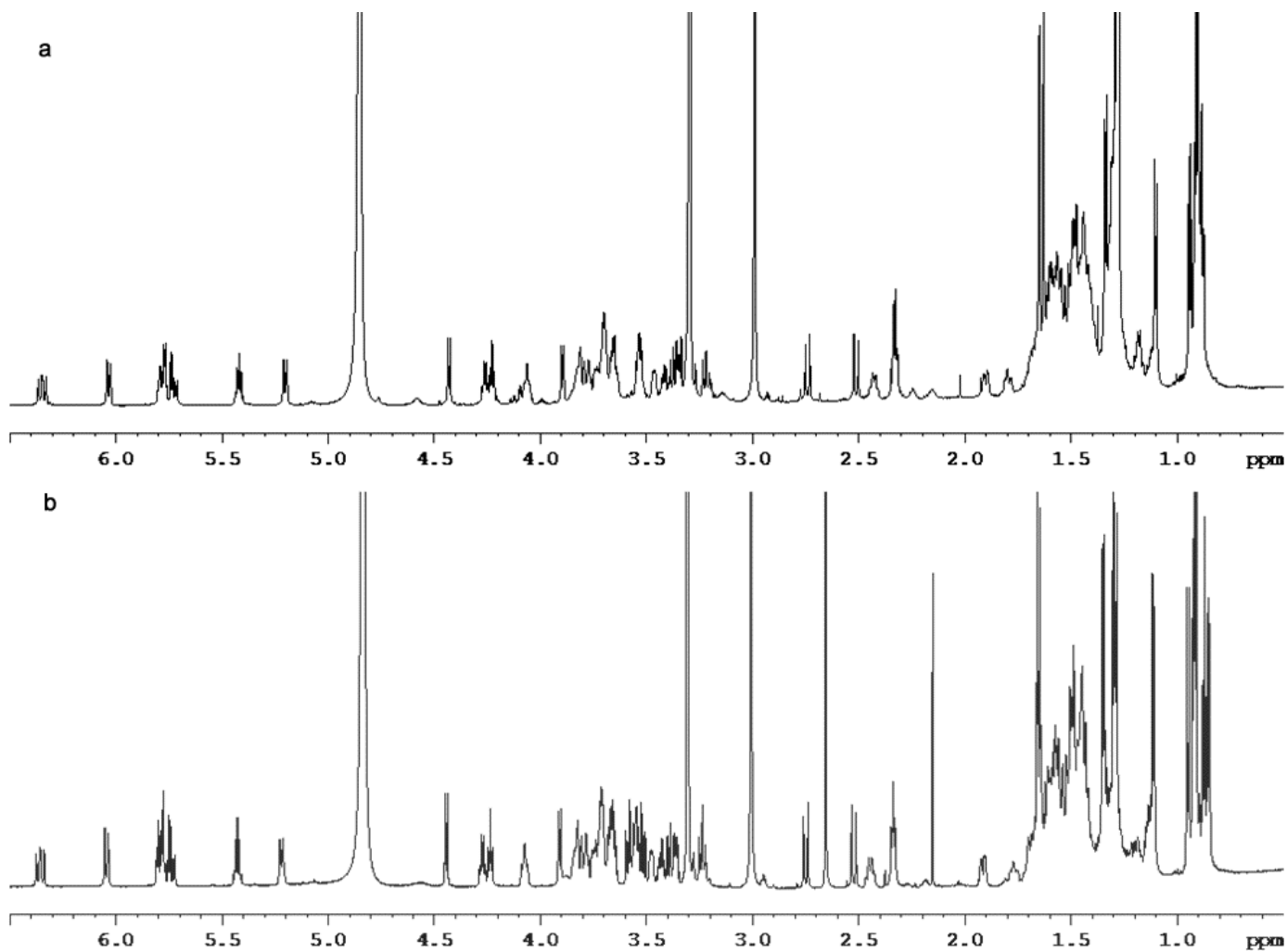
Supplementary Figure 4: Mass spectra from UHPLC-ESI-Q-TOF-MS analysis of methanolic mycelial extracts from the [U-²H]L-isoleucine **9 incorporation experiments.** Spectra resulting from addition of (a) 5 mM [U-²H]L-isoleucine **9** and (b) no [U-²H]L-isoleucine to the growth medium. The signal at $m/z = 700.4757$ corresponds to $[M+Na+H]^{2+}$ for stambomycins A/B **1/2** and the signal at $m/z = 704.5016$ corresponds to $[M+Na+H]^{2+}$ for stambomycin A **1** derived from incorporation of [U-²H]L-isoleucine **9** (calculated for $[C_{73}H_{125}D_9NNaO_{22}]^{2+}$:704.4925;). Spectra for stambomycins C/D **3/4** resulting from addition of (c) 5 mM [U-²H]L-isoleucine **9** and (d) no [U-²H]L-isoleucine to the growth medium. No specific incorporation of the deuterium-labeled precursor is observed.



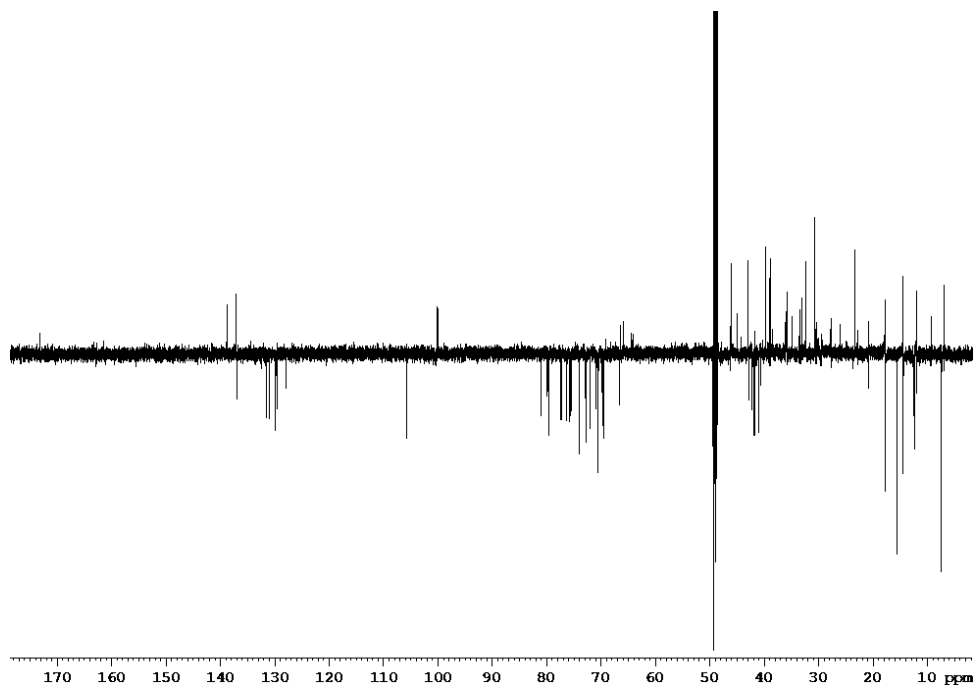
Supplementary Figure 5: Mass spectra from UHPLC-ESI-Q-TOF-MS analysis of methanolic mycelial extracts from the [U-²H]L-leucine 10 incorporation experiments. Spectra resulting from addition of (a) 5 mM [U-²H]L-leucine 10 and (b) no [U-²H]L-leucine to the growth medium. The signal at $m/z = 699.9645$ corresponds to $[M+Na+H]^{2+}$ for stambomycins A/B 1/2 and the signal at $m/z = 704.4945$ corresponds to $[M+Na+H]^{2+}$ for stambomycin B 2 derived from incorporation of [U-²H]L-isoleucine 10 (calculated for $[C_{73}H_{125}D_9NNaO_{22}]^{2+}$:704.4925). Spectra for stambomycins C/D 3/4 resulting from addition of (c) 5 mM [U-²H]L-leucine 10 and (d) no [U-²H]L-leucine to the growth medium. No specific incorporation of the deuterium-labeled precursor was observed. The regions of the spectra highlighted by the blue boxes result from the incorporation of deuterium labeled acetyl-CoA derived from the catabolism of [U-²H]L-leucine 10.



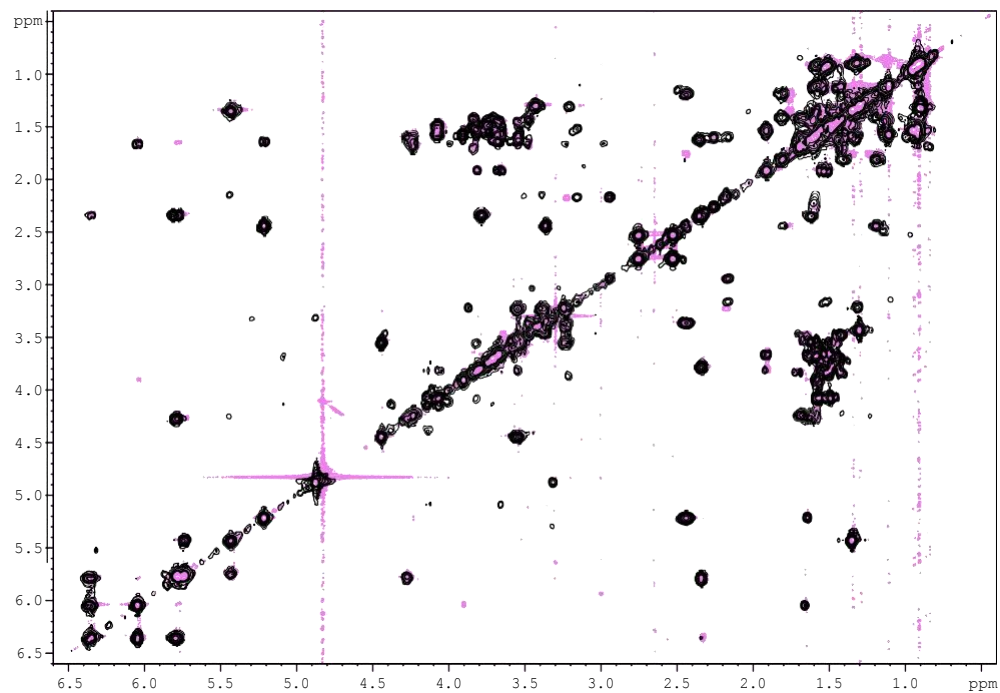
Supplementary Figure 6: UHPLC-ESI-Q-TOF-MS analysis of methanolic mycelial extracts from the *n*-heptanoic acid incorporation experiments. Extracted ion chromatogram at $m/z = 685.9$, corresponding to $[M+Na+H]^{2+}$ for stambomycin analogue **22**, from UHPLC-ESI-Q-TOF-MS analyses of methanolic mycelial extracts *S. ambofaciens* W130 grown in the absence (a) and (b) presence of 5 mM *n*-heptanoic acid. (c) Mass spectrum of **22** from UHPLC-ESI-Q-TOF-MS analyses of *S. ambofaciens* W130 fed with *n*-heptanoic acid. (d) Simulated spectrum for $C_{71}H_{130}NNaO_{22}^{2+}$.



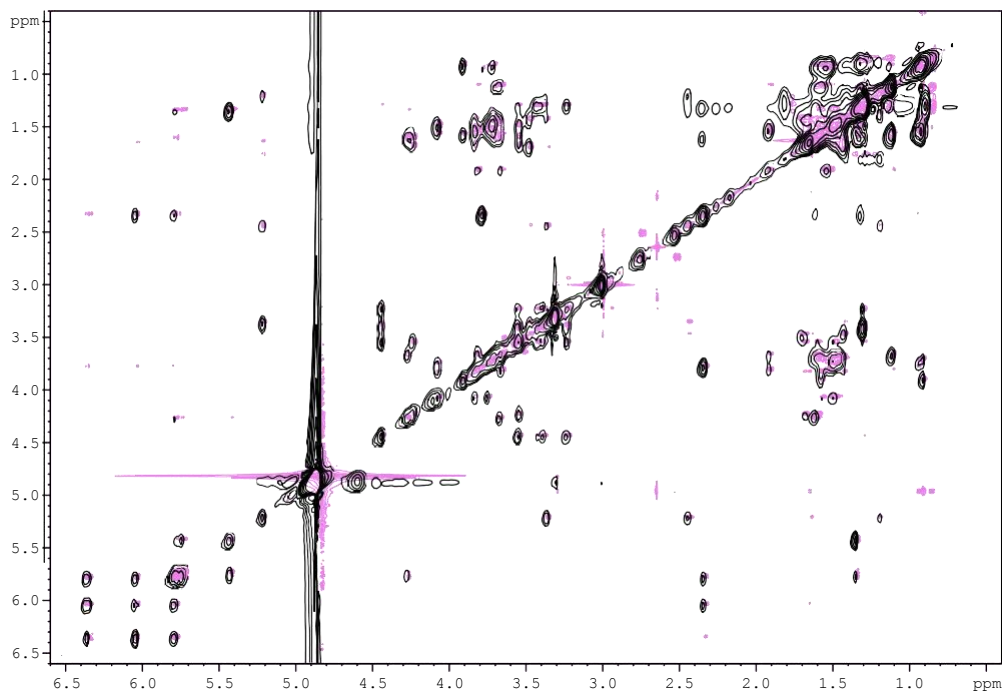
Supplementary Figure 7: Comparison of the ¹H NMR spectra (700 MHz, d₄-MeOH) of (a) 22 and (b) stambomycins C/D 3/4.



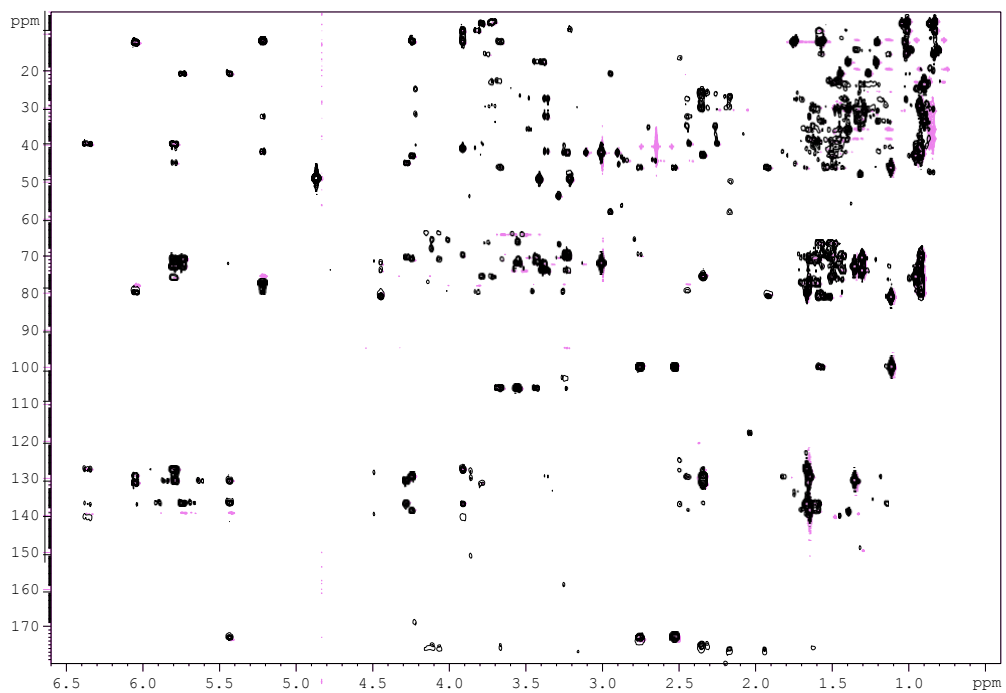
Supplementary Figure 8: ^{13}C -APT NMR spectrum (175 MHz, $\text{d}_4\text{-MeOH}$) of 22.



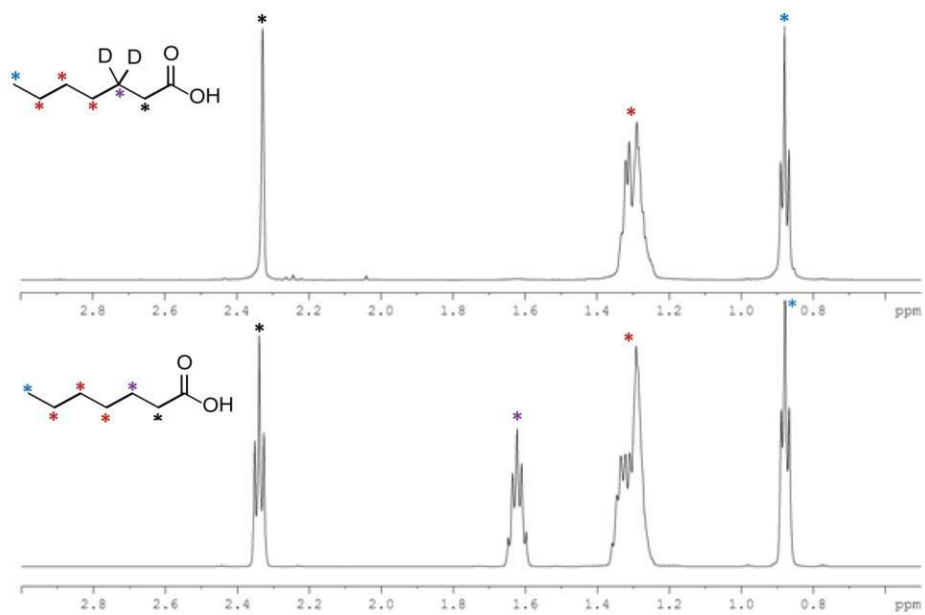
Supplementary Figure 9: Overlaid COSY NMR spectra (700 MHz, d₄-MeOH) of 22 (black) and stambomycins C/D 3/4 (pink).



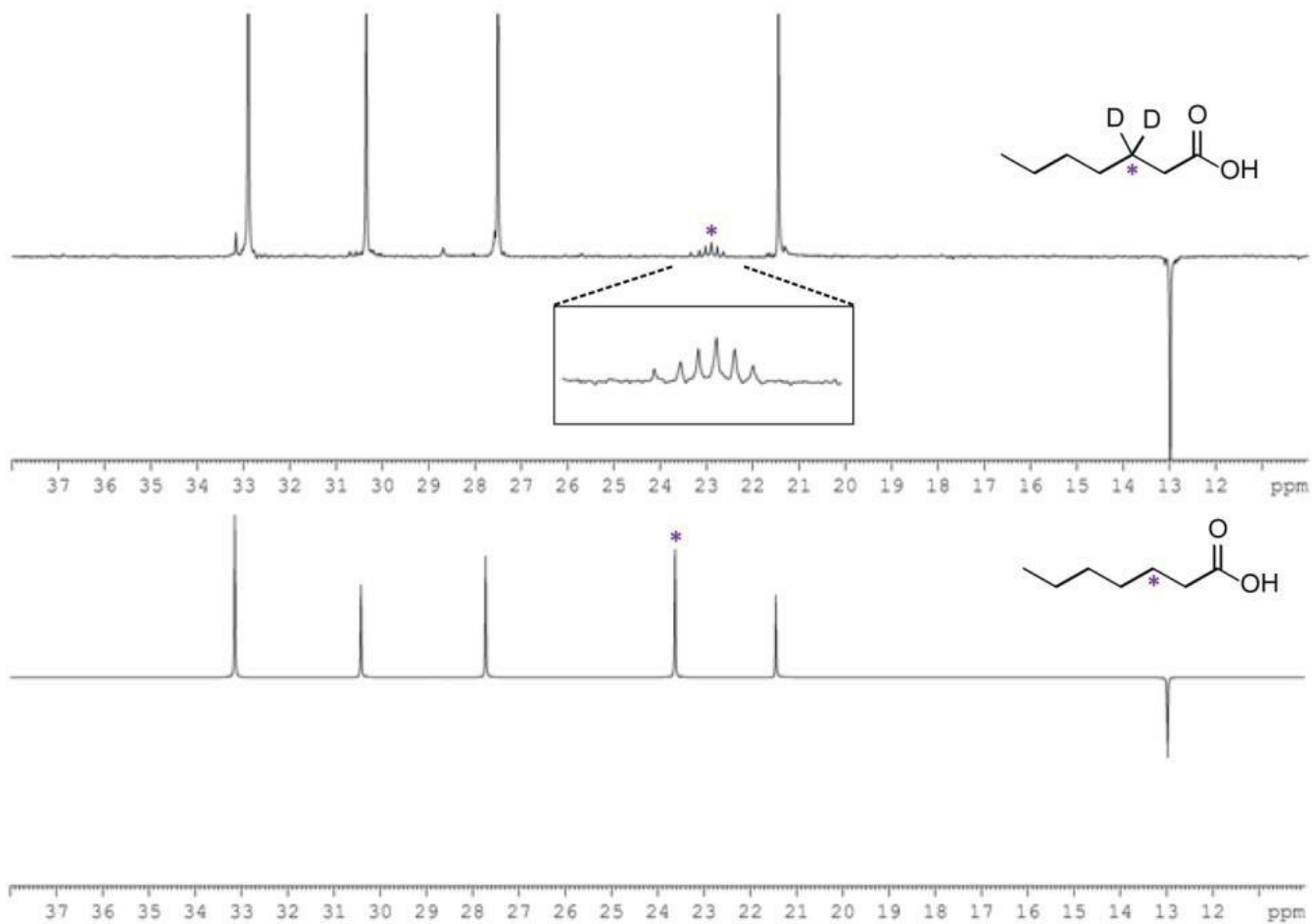
Supplementary Figure 10: Overlaid TOCSY NMR spectra (700 MHz, d_4 -MeOH) of 22 (black) and stambomycins C/D 3/4 (pink).



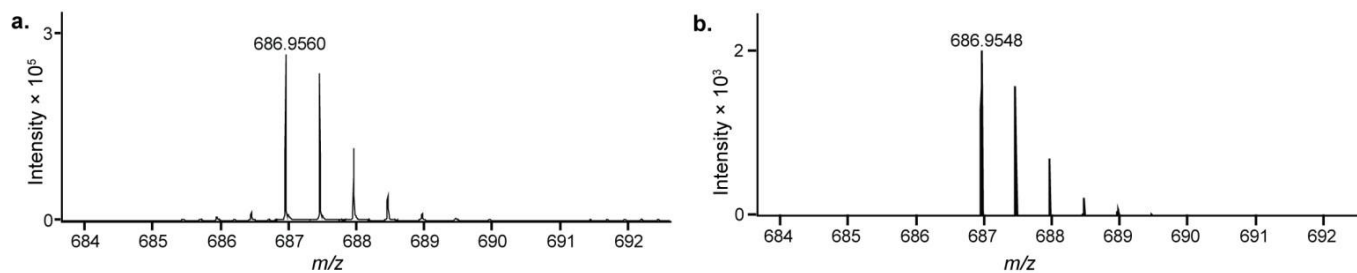
Supplementary Figure 11: Overlaid HMBC NMR spectra (700 MHz / 175 MHz, d₄-MeOH) of 22 (black) and stambomycins C/D 3/4 (pink).



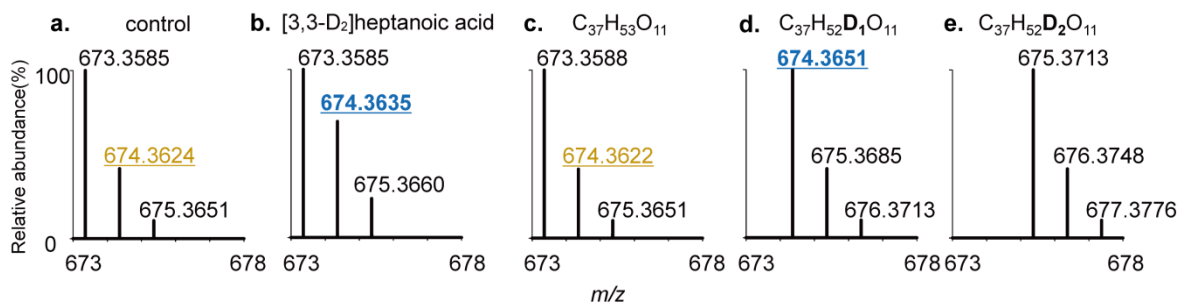
Supplementary Figure 12: Comparison of the ¹H NMR spectra of [3-²H₂]heptanoic acid 23 and unlabeled *n*-heptanoic acid 21.



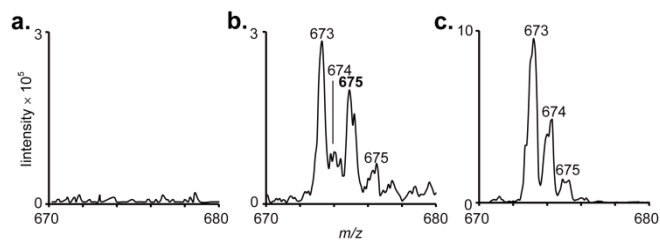
Supplementary Figure 13: Comparison of the ¹³C NMR spectra of [3-²H₂]heptanoic acid 23 and unlabelled *n*-heptanoic acid 21. The splitting of the C-3 signal as a result of the attached deuterium atoms is shown in the inset.



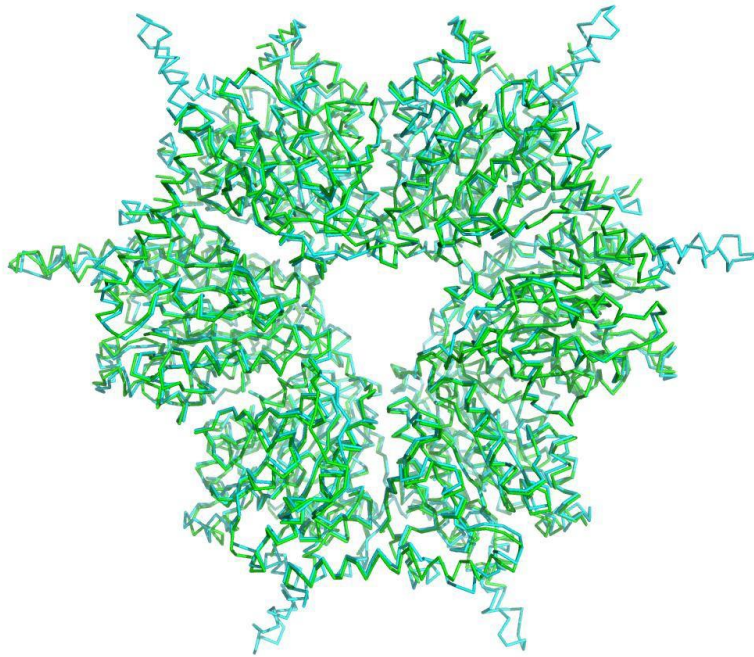
Supplementary Figure 14: Mass spectra from UHPLC-ESI-Q-TOF-MS analysis of the stambomycin analogue **22 produced as a result of feeding [3- $^2\text{H}_2$]heptanoic acid to *S. ambifaciens* W130. (a) Measured spectrum. (b) Simulated spectrum for $\text{C}_{71}\text{H}_{128}\text{D}_2\text{NNaO}_{22}^{2+}$ corresponding to $[\text{M}+\text{Na}+\text{H}]^+$ for doubly labeled **22**.**



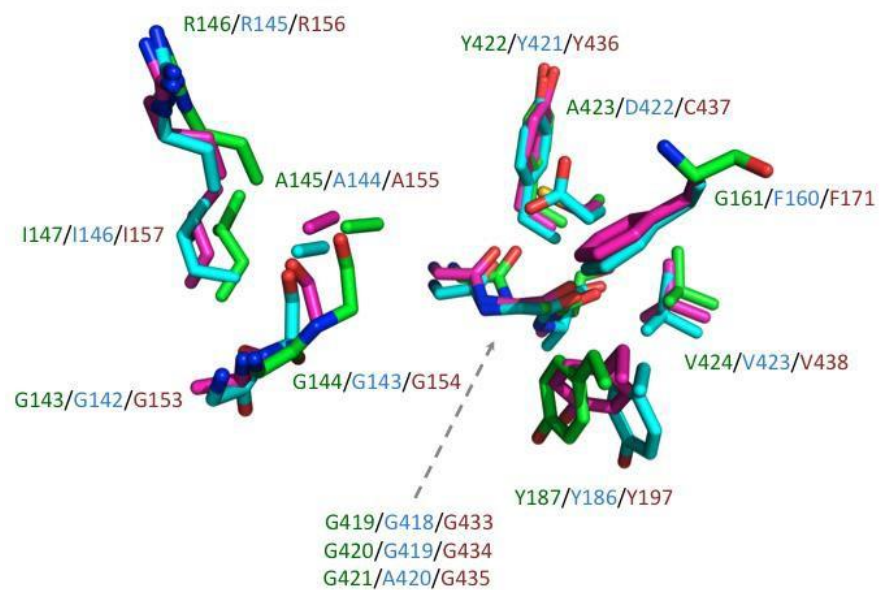
Supplementary Figure 15: Mass spectra from ESI-TOF-MS analysis of partially purified reveromycin D 32 produced from [3- 2H_2]heptanoic acid incorporation experiments. Comparison of ESI-TOF mass spectra of partially purified reveromycin D 32 from cultures of *Streptomyces* sp. SN-593 $\Delta revR$ mutant grown in the absence (a) and presence (b) of [3- 2H_2]heptanoic acid. Simulated isotope distributions for unlabeled (c), singly-labeled (d) and doubly-labeled reveromycin D (e). The data are consistent with 20% incorporation of singly-labeled heptanoic acid into 32.



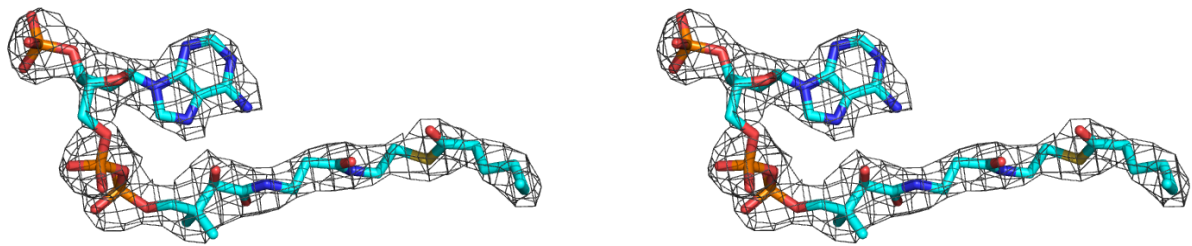
Supplementary Figure 16: LC-MS analysis of partially purified extracts from the [3-²H₂]heptanoic acid incorporation experiments. Mass spectra of reveromycin D **32** from LC-MS analyses of partially purified extracts from the cultures of (a) the $\Delta revT$ mutant, (b) the $\Delta revT::samR0483$ mutant to which [3-²H₂]heptanoic acid **23** has been fed, and (c) wild type *Streptomyces* sp. SN-593.



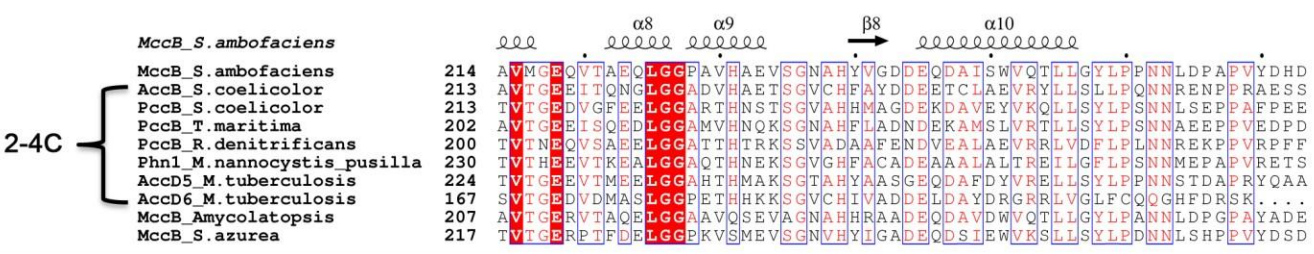
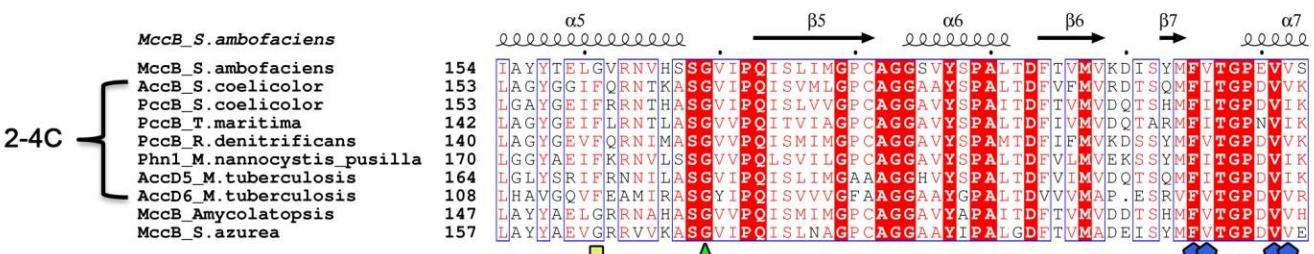
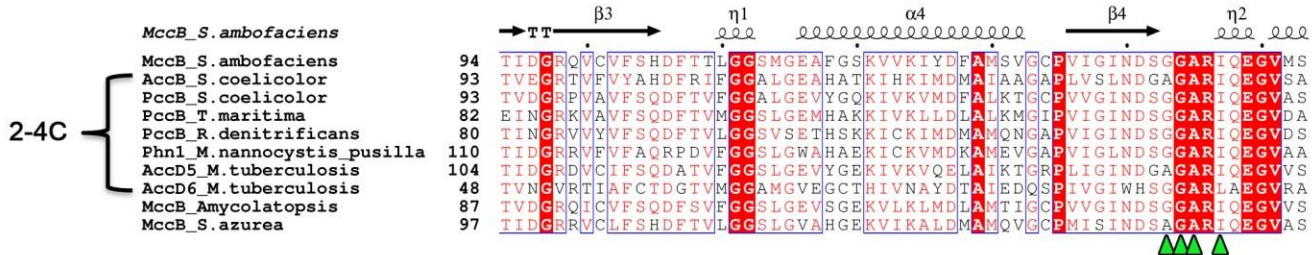
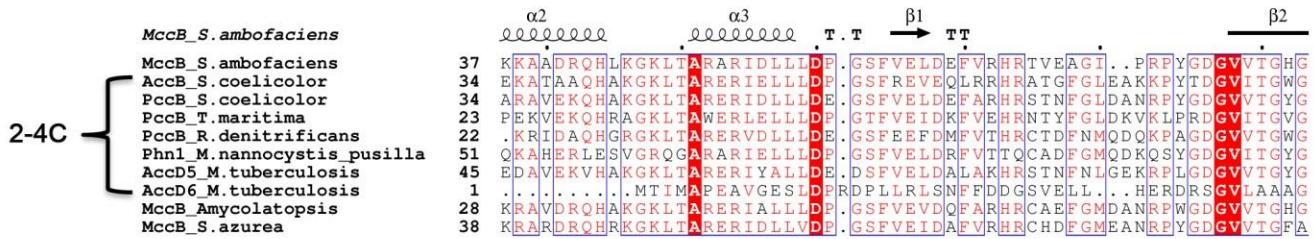
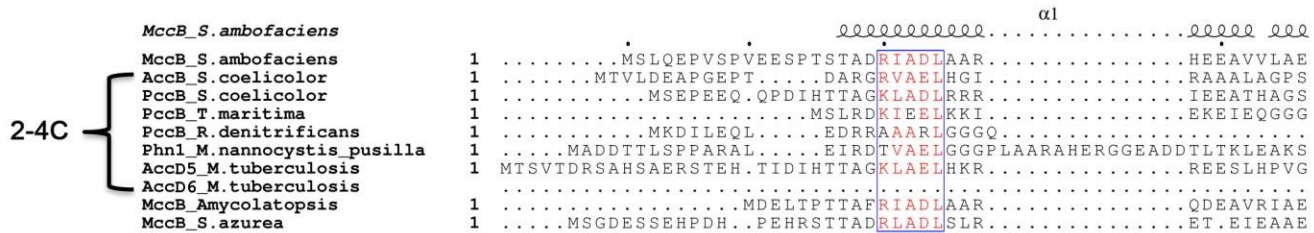
Supplementary Figure 17: Superimposition of PccB from *S. coelicolor* (cyan) with MccB from *S. ambofaciens* (green). The structures are displayed as colored ribbons.

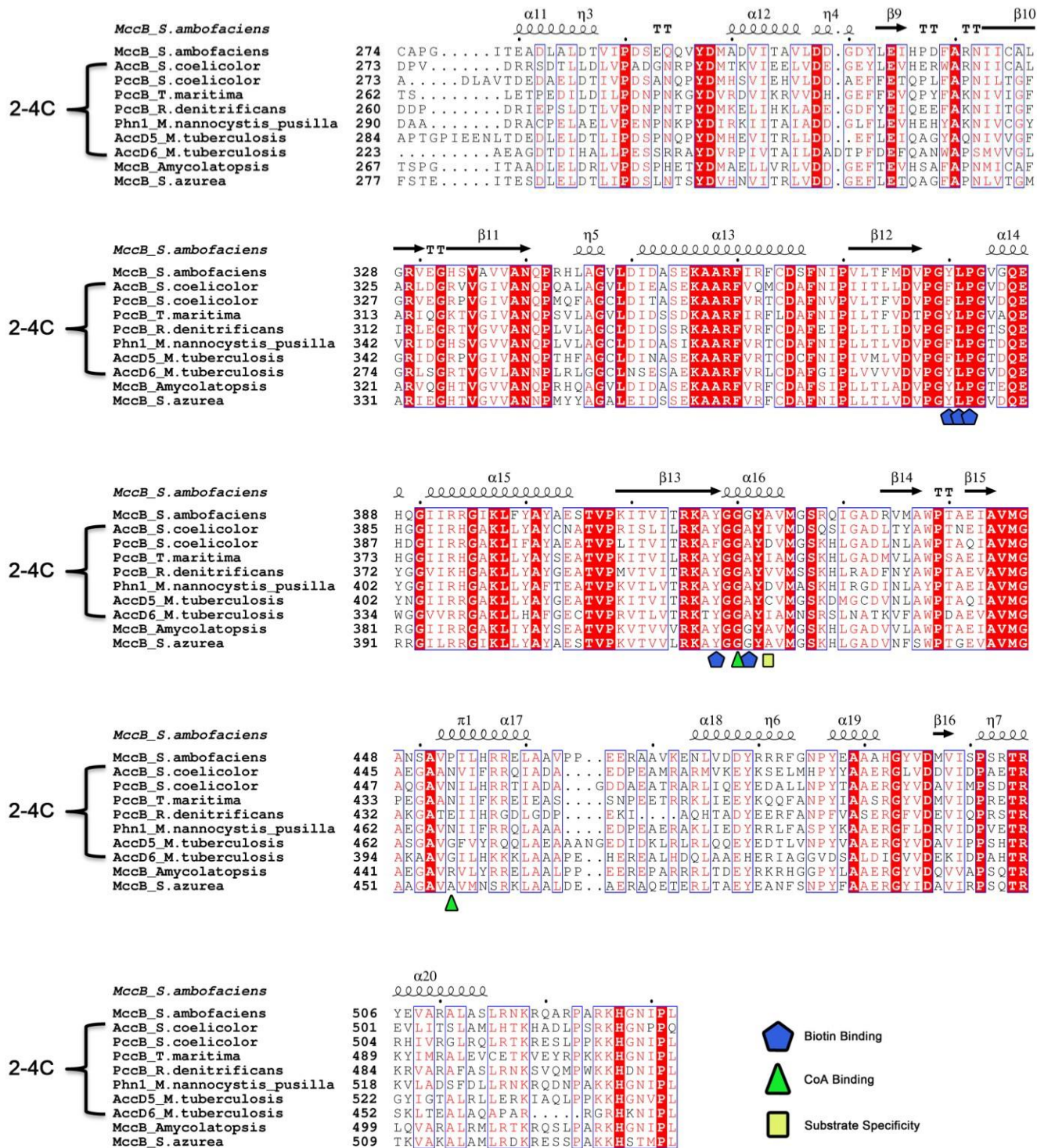


Supplementary Figure 18: Structural comparison of MccB (PDB ID: 5INI), PccB (PDB ID: 1XNY), and AccD5 (PDB ID: 2A7S) active site residues. Colors are green, cyan, and magenta, respectively.

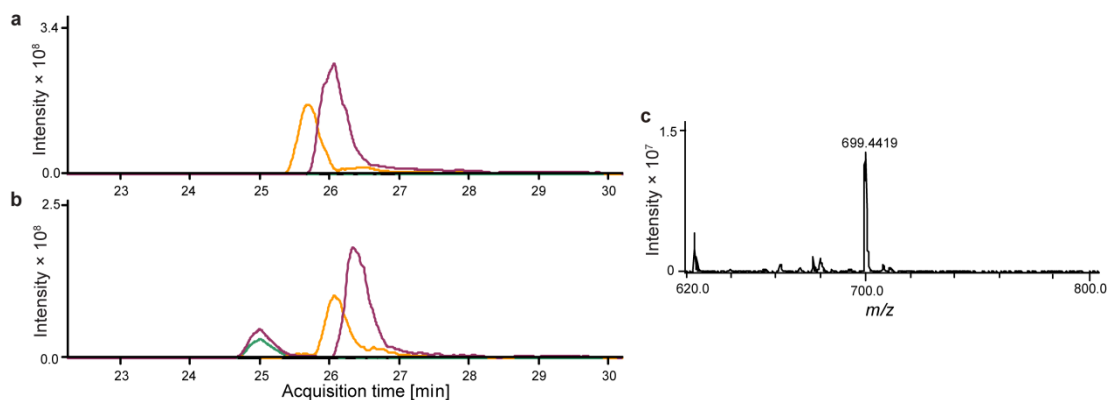


Supplementary Figure 19: Stereo view of hexanoyl-CoA bound to MccB with 2F0-FC SA omit map contoured 1.0 σ at 2.85 Å. The surrounding protein has been removed for clarity.

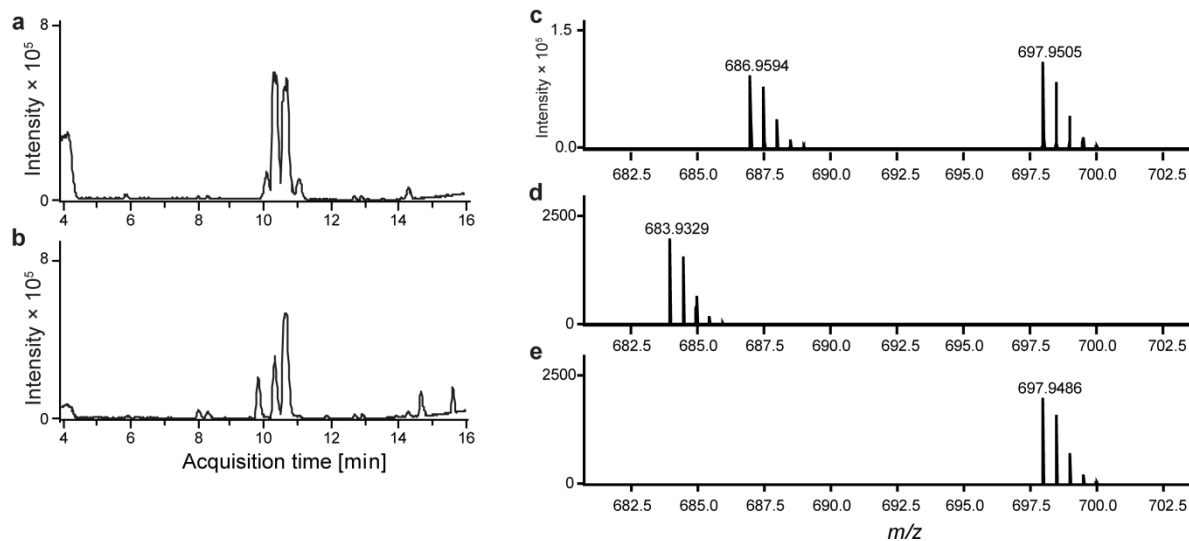




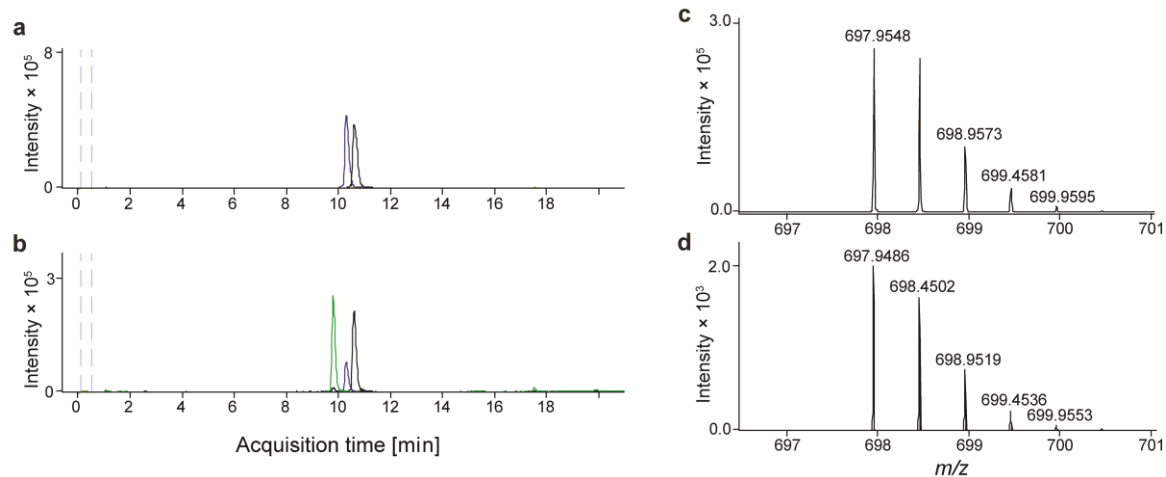
Supplementary Figure 20: Sequence alignment of MccB from *S. ambofaciens* with other ACC β -subunits. The enzymes denoted 2-4C use acetyl-, propionyl or butyryl-CoA as a substrate. MccB in *Streptomyces azurea* is proposed to assemble butylmalonyl-CoA and other 6-8 carbon extender units incorporated by PriA6 into the primycins.⁹



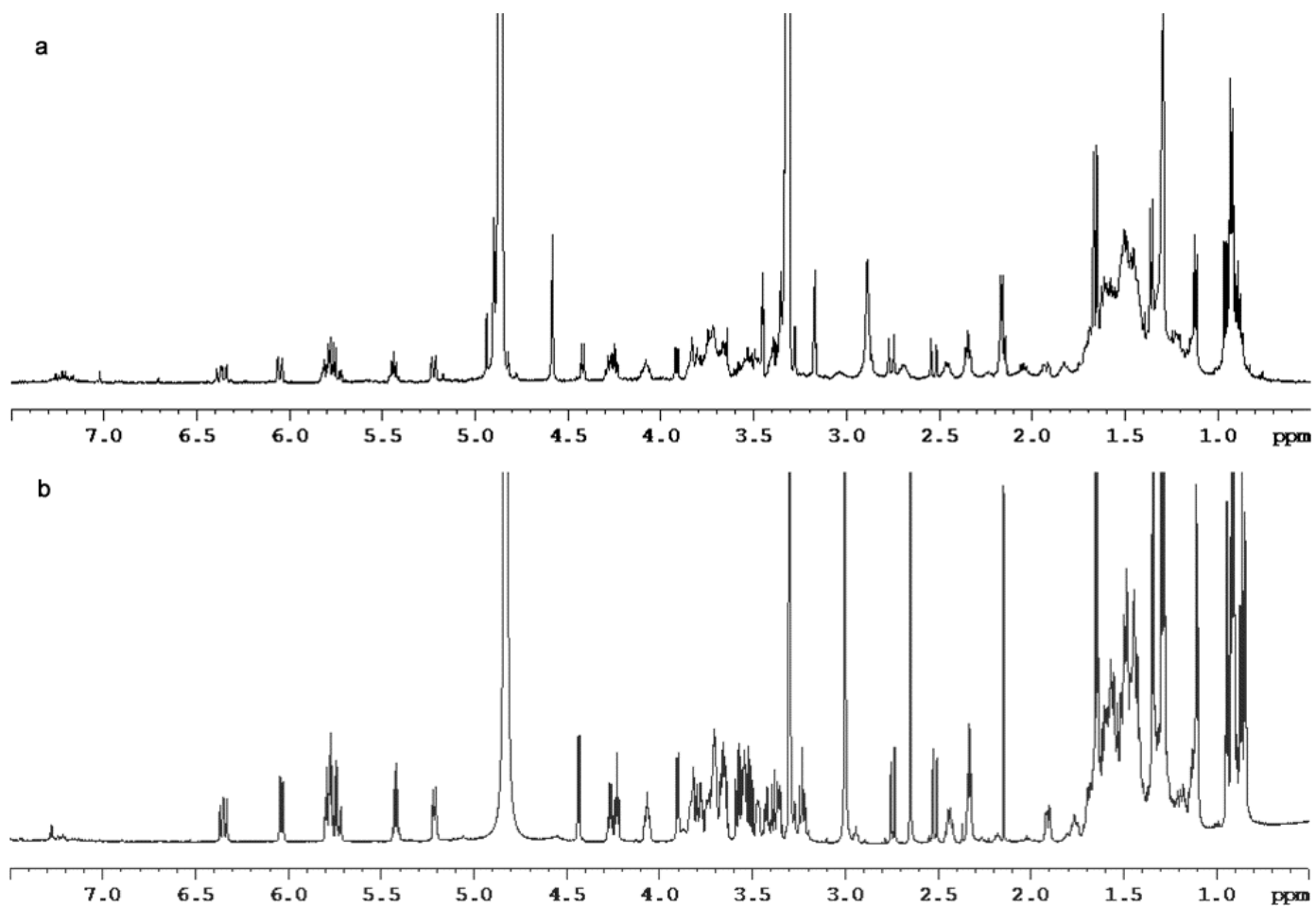
Supplementary Figure 21: UHPLC-ESI-Q-TOF-MS analysis of methanolic mycelial extracts from the 6-azidohexanoic acid incorporation experiments. EICs at $m/z = 699.4$, corresponding to $[M+H+Na]^{2+}$ for stambomycin analogue **37** (green), at $m/z = 692.9$, corresponding to $[M+H+Na]^{2+}$ for stambomyces C/D **3/4** (orange), and at $m/z = 699.9$, corresponding to $[M+H+Na]^{2+}$ for stambomyces A/B **1/2** (purple), from UHPLC-ESI-Q-TOF-MS analyses of methanolic mycelial extracts of *S. ambofaciens* W130 grown in the absence (**a**) and presence (**b**) of 5 mM 6-azidohexanoic acid. (**c**) Measured mass spectrum for peak corresponding to stambomycin analogue **37** with a retention time of 25 minutes (calculated for $C_{70}H_{127}N_4NaO_{22}^+$: 699.4414).



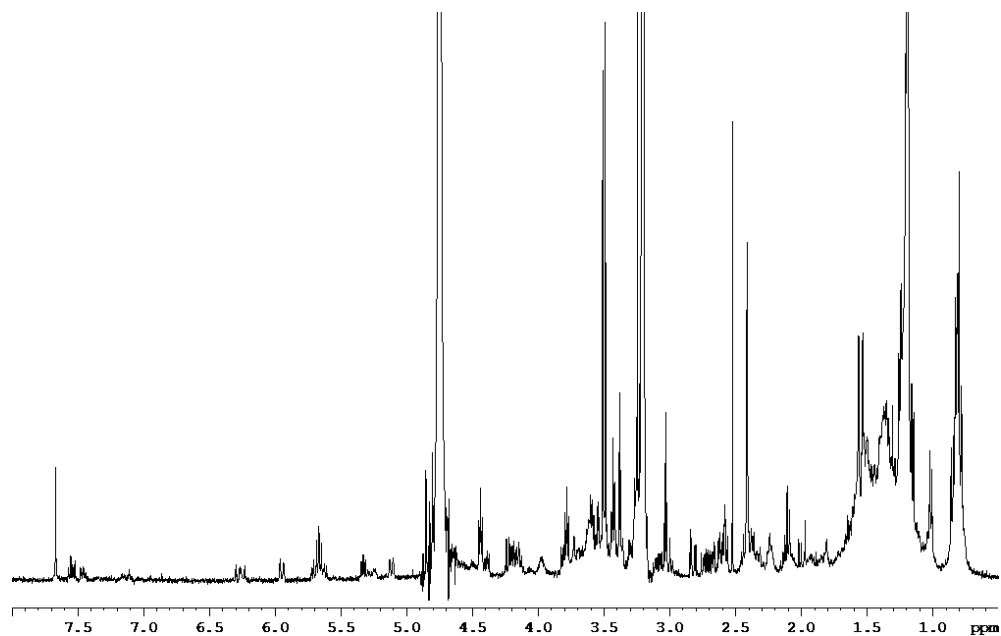
Supplementary Figure 22: UHPLC-ESI-Q-TOF-MS analysis of methanolic mycelial extracts from the 6-heptynoic acid incorporation experiments. Base peak chromatograms from UHPLC-ESI-Q-TOF-MS analyses of mycelial extracts of *S. ambofaciens* W130 grown in the absence (a) and presence (b) of 5 mM 6-heptynoic acid. The peaks with retention times of 10.3 minutes and 10.7 minutes correspond to stambomycins C/D **3/4** and stambomycins A/B **1/2**, respectively. A new peak with a retention time of 9.8 minutes, corresponding to a novel stambomycin analogue is observed. (c) Mass spectrum of the stambomycin analogue with a retention time of 9.8 minutes observed in UHPLC-ESI-Q-TOF-MS analyses of *S. ambofaciens* W130 fed with 6-heptynoic acid. (d) Simulated spectrum for $C_{71}H_{126}NNaO_{22}^{2+}$, corresponding to the stambomycin analogue expected to result from direct incorporation of 6-heptynoic acid. (e) Simulated spectrum for $C_{73}H_{130}NNaO_{22}^{2+}$, corresponding to stambomycin analogue **39**.



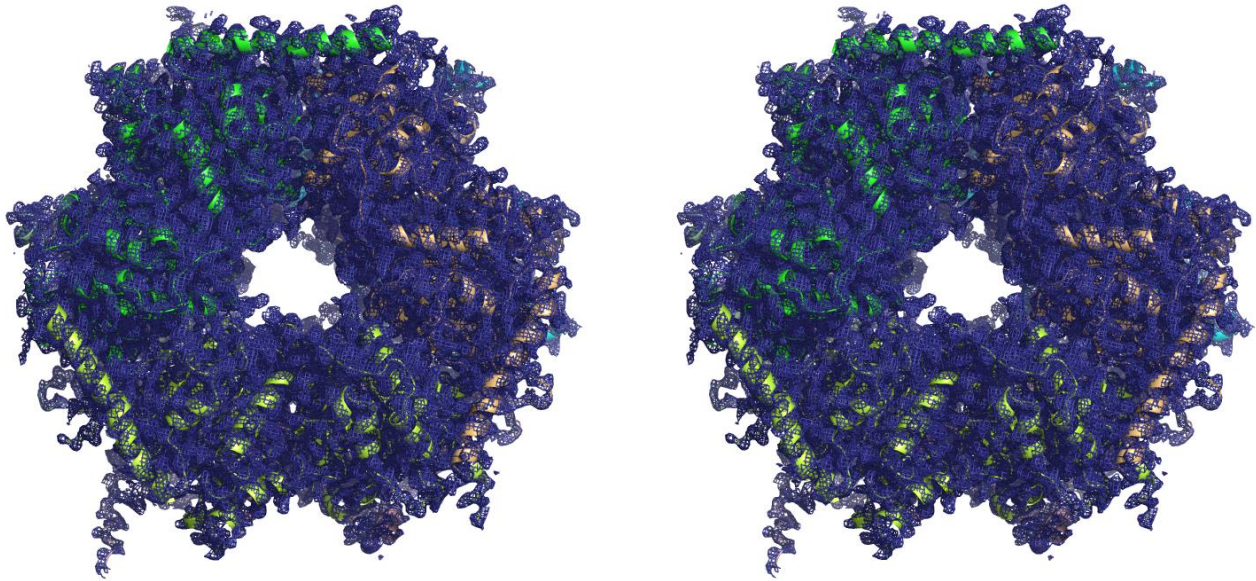
Supplementary Figure 23: UHPLC-ESI-Q-TOF-MS analysis of methanolic mycelial extracts from the 8-nonynoic acid incorporation experiments. EICs at $m/z = 697.9$, corresponding to $[M+H+Na]^{2+}$ for stambomycin analogue **39** (green), at $m/z = 692.9$, corresponding to $[M+H+Na]^{2+}$ for stambomycins C/D **3/4** (blue), and at $m/z = 699.9$, corresponding to $[M+H+Na]^{2+}$ for stambomycins A/B **1/2** (black), from UHPLC-ESI-Q-TOF-MS analyses of methanolic mycelial extracts of *S. ambofaciens* W130 grown in the absence (a) and presence (b) of 5 mM 8-nonynoic acid. (c) Measured and (d) simulated mass spectra for the $[M+Na+H]^{2+}$ ion of stambomycin analogue **39**.



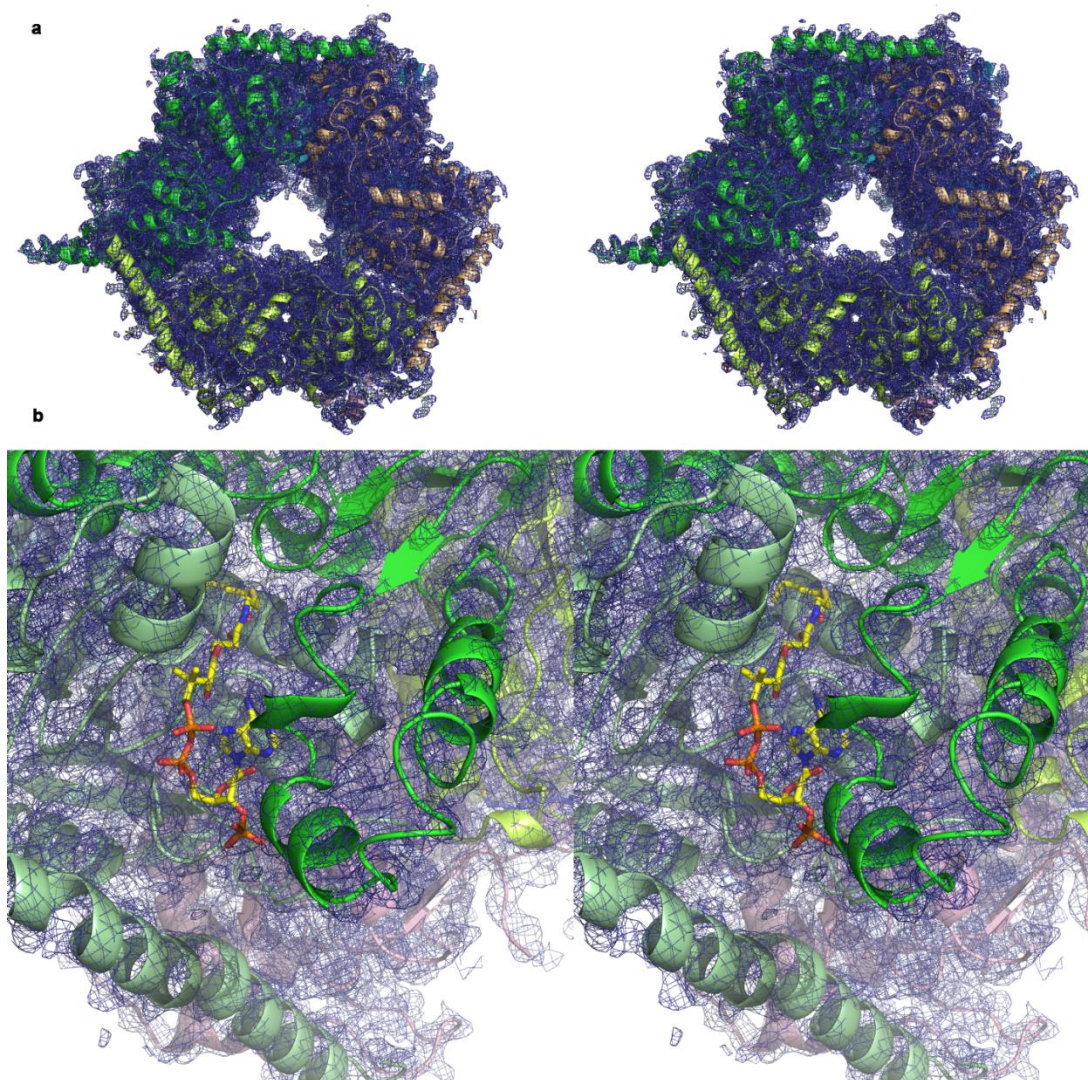
Supplementary Figure 24: Comparison of ¹H-NMR spectra (600 MHz, MeOD) for (a) stambomycin analogue 39 and (b) stambomycins C/D 3/4 .



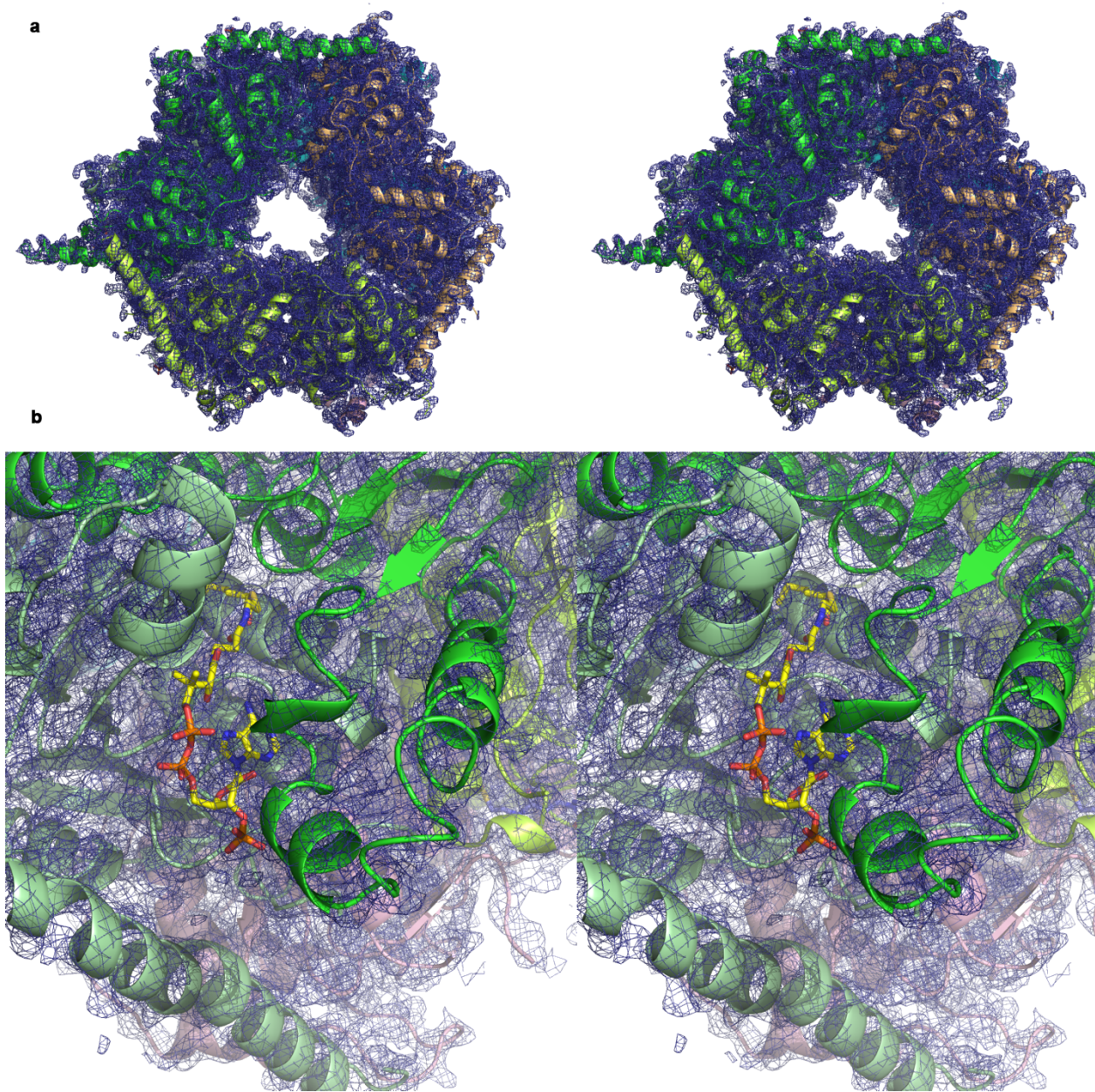
Supplementary Figure 25: ¹H-NMR (400 MHz, MeOD) spectrum of biotinylated stambomycin analogue derived from the click reaction of stambomycin analogue 39 with the azide-PEG3-biotin conjugate. The signal at 7.68 ppm corresponds to the triazole proton and the signals at 4.2 ppm correspond to the protons around the fused thiolane ring of biotin.



Supplementary Figure 26: Stereo view of the apo-MccB hexamer with 2F0-FC map contoured to 1.0σ at 2.45 Å.



Supplementary Figure 27: Stereo views of the MccB hexamer bound to four molecules of hexanoyl-CoA. (a) The overall architecture of MccB bound to four molecules of hexanoyl-CoA. **(b)** The active site pocket at the dimer interface of opposing MccB monomers. 2F0-FC maps are contoured to 1.0σ at 2.85 \AA .



Supplementary Figure 28: Stereo views of the MccB hexamer bound to one molecule of hexanoyl-CoA. (a) The overall architecture of MccB bound to one molecule of hexanoyl-CoA. **(b)** The active site pocket at the dimer interface of opposing MccB monomers. 2F₀-F_c maps are contoured to 1.0 σ at 2.75 Å.

Supplementary Table 1: Bacterial strains and plasmids

Strain/plasmid	Relevant characteristics	Ref.
Strain		
<i>S. ambifaciens</i> ATCC 23877	Wild-type strain, in which stambomycin cluster is poorly expressed	4
<i>S. ambifaciens</i> W130	Stambomycin producing strain in which <i>samR0484</i> is integrated into the chromosome and is under control of the <i>ermE*</i> promoter	This work
<i>E. coli</i> ET12567/pUZ8002	Strain used for conjugal transfer of pOSV556t derivatives into <i>S. ambifaciens</i> ATCC 23877	5
<i>Streptomyces</i> sp. SN-593	Wild-type reveromycin-producing strain	6
<i>E. coli</i> GM2929 <i>hsdS</i> ::Tn10 / pUB307- <i>aph</i> ::Tn7	Strain used for conjugal transfer of pTYM19 derivatives into <i>Streptomyces</i> sp. SN-593	7
$\Delta revT$	<i>revT</i> disruptant of <i>Streptomyces</i> sp. SN-593	8
$\Delta revR$	<i>revR</i> disruptant of <i>Streptomyces</i> sp. SN-593	8
$\Delta revT$:: <i>samR0483</i>	$\Delta revT$ mutant complemented with pTYM19- <i>P_{aph}</i> - <i>samR0483</i>	This work
Plasmid		
pOSV556t	Integrative <i>E. coli</i> - <i>Streptomyces</i> shuttle vector	9
pOSV556t- <i>samR0484</i>	<i>samR0484</i> inserted between the <i>Hind</i> III and <i>Cl</i> I sites of pOSV556t	This work
pOSV556t- <i>samR0483</i>	<i>samR0483</i> inserted between the <i>Hind</i> III and <i>Cl</i> I sites of pOSV556t	This work
pTYM19	Integrative <i>Streptomyces</i> - <i>E. coli</i> shuttle vector	10
pTYM19- <i>P_{aph}</i>	Derivative of pTYM19 in which the <i>aph</i> II promoter fragment is inserted into the <i>Eco</i> RI and <i>Bam</i> HI sites.	11
pTYM19- <i>P_{aph}</i> - <i>samR0483</i>	<i>samR0483</i> inserted into <i>Bam</i> HI and <i>Hind</i> III sites of pTYM19- <i>P_{aph}</i>	This work
pET151- <i>samR0483</i>	MccB overproduction construct	This work
pET28a- <i>samR0483</i>	MccB overproduction construct	This work

Supplementary Table 2: Oligonucleotide primers

Target gene (template)	Primers	Ref.
<i>samR0484</i>	pOSV_samR0484_FW: 5'-AAAGGGAAGCTTAGGAGGCCAGTCATTGCTGGTCC-3'	This work
(for cloning into pOSV556t between <i>HindIII</i> and <i>Clal</i>)	pOSV_samR0484_RV: 5'-CCCTTTATCGATCGTGGGCAGGCTCTGCTC-3'	
<i>samR0483</i>	pOSV_samR0483_FW: 5'-AAGGGAAGCTTGCTGGTATGTCGTCCCA-3'	This work
(for cloning into pOSV556t between <i>HindIII</i> and <i>Clal</i>)	pOSV_samR0483_RV: 5'-CCCTTTATCGATACGACGTCACA-3'	
<i>samR0483</i>	0483_BamHI: 5'-CGCGGATCCATGTCGCTCCAGGA-3'	This work
(pOSV556t- <i>samR0483</i>)	0483_HindIII: 5'-GGGAAGCTTTCACAGGGGAATGT-3'	
<i>samR0483</i>	TOPO_483_FW: 5'-CACCATGTCGCTCCAGGAGCCTGTCTC-3'	This work
(For TOPO cloning into pET151)	TOPO_483_R: 5'-TCACAGGGGAATGTTCCCGTGTT-3'	
<i>samR0483</i> in <i>pET151</i>	pET28a-samR0483_FW: 5'-ATGCGCGCTAGCGATTCTACGGAAAAC-3'	This work
(For cloning into pET28a between <i>NheI</i> and <i>NotI</i>)	pET28a-samR0483_RV: 5'-TATATAGCGGCCGCTCACAGGGGAATGTT-3'	

Supplementary Table 3: Comparison of ^1H and ^{13}C NMR data for stambomycin D¹ (**4**) and stambomycin analogue **22**. The atom numbering is shown in Figure 3 of the main manuscript.

Position	δ_{C} (ppm) in 4	δ_{C} (ppm) in 22	δ_{H} (ppm) in 4	δ_{H} (ppm) in 22	$J_{\text{H-H}}$ (Hz)
1	173.3	173.1	-	-	
2	44.3	44.3	2.52, 2.83	2.53, 2.76	14.5
3	100.0	100.1	-	-	
4	46.2	46.2	1.56	1.57	
4-Me	12.4	12.5	1.04	1.11	
5	81.0	81.0	3.66	3.66	
1'	104.6	105.8	4.44	4.44	7.0
2'	70.0	69.8	3.54	3.54	7.5, 10.5
3'	72.0	72.0	3.23	3.23	10.5
4'	70.8	70.5	3.38	3.39	10.0
5'	74.0	74.0	3.42	3.42	6.0, 9.0
6'	18.1	17.8	1.29	1.29	
3'-NMe ₂	42.2	42.3	3.03	3.00	
6	39.1	38.9	1.61, 1.90	1.91	
7	70.0	69.9	3.83	3.83	
8	40.8	41.0	1.56	1.58	
8-Me	9.3	9.4	0.93	0.89	
9	79.9	79.9	3.90	3.90	7.5
10	137.1	136.9	-	-	
10-Me	12.4	12.4	1.65	1.65	
11	128.0	127.8	6.06	6.04	11.0
12	129.9	129.5	6.35	6.36	11.0, 14.5
13	131.7	131.6	5.81	5.80	
14	39.8	39.8	2.34	2.34	6.5
15	75.8	75.7	3.77	3.78	
16	42.6	42.9	1.52	1.52	
16-Me	7.4	7.4	0.95	0.96	
17	75.5	75.5	3.72	3.72	
18	36.1	36.1	1.48	1.47	
19	23.5	23.3	1.32, 1.34	1.32	
20	38.5	38.5	1.47	1.45	
21	71.1	70.9	3.55	3.55	
22	43.1	43.0	1.61, 1.67	1.61, 1.68	
23	77.5	77.4	4.23	4.23	7.0
24	139.4	138.5	-	-	
24-Me	12.2	12.4	1.64	1.64	
25	129.3	129.9	5.23	5.21	10.5

26	41.9	41.8	2.45	2.44	
1"	32.4	32.4	1.18, 1.79	1.19, 1.81	7.0
2"	26.6	30.6	1.37	1.38	
3"	35.8	34.9	1.31, 1.44	1.29	
4"	34.0	33.0	1.43, 1.49	1.28	
5"	29.2	14.4	1.29	0.88	
6"	11.5	-	0.87	-	
27	79.7	79.6	3.36	3.36	
28	74.2	74.0	3.47	3.47	
29	27.8	27.8	1.43, 1.68	1.42, 1.66	
30	36.1	36.0	1.43, 1.70	1.69	
31	70.1	69.9	3.83	3.83	
32	46.4	46.2	1.50, 1.57	1.51, 1.57	
33	66.8	66.7	4.06	4.07	
34	42.0	41.8	1.48, 1.50	1.49, 1.50	
35	72.9	72.8	3.74	3.74	
36	40.8	40.6	1.48	1.47	
36-Me	15.6	15.6	0.92	0.93	
37	29.8	29.6	1.28, 1.12	1.12, 1.56	
38	36.0	36.0	1.50	1.49	
39	76.3	76.3	3.72	3.72	
40	42.3	42.3	1.51	1.51	
40-Me	7.0	6.9	0.91	0.92	
41	75.9	75.9	3.71	3.71	
42	33.8	33.6	1.43, 1.62	1.43, 1.62	
43	22.9	22.9	1.43	1.45	
44	38.8	38.9	1.45, 1.46	1.45, 1.46	
45	70.6	70.5	3.67	3.67	
46	44.8	44.9	1.60, 1.65	1.60	
47	71.1	71.0	4.28	4.27	6.5, 13.0
48	136.7	136.8	5.80	5.77	5.0, 10.5
49	130.8	130.9	5.72	5.73	6.0, 15.5
50	72.8	72.8	5.43	5.42	6.0
51	20.8	20.8	1.33	1.35	

Supplementary Table 4: Crystallographic statistics

	apo-Mccb	Mccb + 1 Hex-CoA	Mccb + 4 Hex-CoA
	5ING	5INF	5INI
Data collection	ALS BL821	ALS BL822	ALS BL821
Wavelength (Å)	0.9999	0.9998	1.000
Space group	P2 ₁ 2 ₁ 2 ₁	P2 ₁ 2 ₁ 2 ₁	P2 ₁ 2 ₁ 2 ₁
Cell dimensions			
<i>a</i> , <i>b</i> , <i>c</i> (Å)	120.56, 163.44, 186.55	110.072 165.453	110.978,161.526, 187.294
α , β , γ (°)	90, 90, 90	90, 90, 90	90, 90, 90
Resolution (Å)	58.12 - 2.45	42.22 - 2.75	48.44 - 2.85
<i>R</i> _{merge}	0.112 (0.966)	0.208 (0.837)	0.206 (0.731)
<i>I</i> / σ <i>I</i>	11.8 (1.6)	14.4 (3.5)	10 (3.6)
Completeness (%)	99 (97.3)	100 (99.9)	100 (99.4)
Multiplicity	6.1 (5.4)	7.4 (7.3)	6.9 (6.7)
<i>CC</i> (1/2)	(0.662)	(0.796)	(0.820)
Refinement			
Resolution (Å)	58.12 - 2.45	42.22 - 2.75	48.44 - 2.85
No. reflections	133794 (12965)	90300 (8650)	79173 (7792)
<i>R</i> _{work} / <i>R</i> _{free}	0.195/0.223	0.184/0.242	0.173/0.230
No. atoms			
Protein	22424	21976	22284
Ligand/ion	N/A	55	220
Water	956	1091	392
B-factors			
Protein	48.57	27.71	24.59
Ligand/ion	N/A	52.88	54.39
Water	47.12	26.09	20.27
R.M.S deviations			
Bond lengths (Å)	0.007	0.013	0.007
Bond angles (°)	1.07	1.17	0.90

All structures were determined from a single crystal

*Highest resolution shell is shown in parenthesis.

Supplementary References

1. Quade, N., Huo, L., Rachid, A. Heinz, D.W. & Müller, R. Unusual carbon fixation gives rise to diverse polyketide extender units. *Nat. Chem. Biol.* **8**, 117-124 (2012)
2. Peter, D.M. *et al.* Screening and engineering the synthetic potential of carboxylating reductases from central metabolism and polyketide biosynthesis. *Angew. Chem., Int. Ed.* **54**, 13457-13461 (2015)
3. Zhang, L. *et al.* Rational control of polyketide extender units by structure-based engineering of crotonyl-CoA carboxylase/reductase in antimycin biosynthesis. *Angew. Chem., Int. Ed.* **54**, 13463-13465 (2015)
4. Laureti, L. *et al.* Identification of a bioactive 51-membered macrolide complex by activation of a silent polyketide synthase in *Streptomyces ambofaciens*. *Proc. Natl. Acad. Sci. U. S. A.* **108**, 6258-6263 (2011)
5. Kieser, T., Bibb, M. J., Buttner, M. J. Chater, K. F. & Hopwood, D. A. *Practical Streptomyces Genetics*, John Innes Foundation, Norwich (2000).
6. Osada, H., Koshino, H., Isono, K., Takahashi, H. & Kawanishi, G. Reveromycin A, a new antibiotic which inhibits the mitogenic activity of epidermal growth factor. *J. Antibiot. (Tokyo)* **44**, 259-261 (1991)
7. Komatsu, M., Uchiyama, T., Omura, S., Cane, D. E. & Ikeda, H. Genome-minimized *Streptomyces* host for the heterologous expression of secondary metabolism. *Proc. Natl. Acad. Sci. U. S. A.* **107**, 2646-2651 (2010)
8. Miyazawa, T *et al.* Identification of middle chain fatty acyl-CoA ligase responsible for the biosynthesis of 2-alkylmalonyl-CoAs for polyketide extender unit. *J. Biol. Chem.* **290**, 26994-27011 (2015)
9. Kindly provided by Dr Jean-Luc, Pernodet, Université Paris-Sud 11, Orsay, France.
10. Onaka, H., Taniguchi, S., Ikeda, H., Igarashi, Y. & Furumai, T. pTOYAMAcos, pTYM18, and pTYM19, actinomycete-*Escherichia coli* integrating vectors for heterologous gene expression. *J. Antibiot. (Tokyo)* **56**, 950-956 (2003)
11. Takahashi, S. *et al.* Biochemical characterization of a novel indole prenyltransferase from *Streptomyces* sp. SN-593. *J. Bacteriol.* **192**, 2839-2851 (2010)
12. Hong, H., Samborsky, M., Lindner, F. & Leadlay, P.F. An amidinohydrolase provides the missing link in the biosynthesis of amino marginolactone antibiotics. *Angew. Chem., Int. Ed.* **55**, 1118-1123 (2016)